Electronic Supplementary Material (ESI) for Inorganic Chemistry Frontiers.

Supplementary information

Bifunctional hierarchical core-shell $Mo_2C@ZnIn_2S_4$ Schottky junction for efficient photocatalytic H_2-evolution integrated with valuable furfural-production

*Jian Yang, Xiaorui Zhang, Zikang Zeng, Chuang Han, Yujun Liang**

Engineering Research Center of Nano-Geomaterials of Ministry of Education, Faculty of Materials Science and Chemistry, China University of Geosciences, Wuhan 430074, China.

***Corresponding author:** Tel.: +86 27 67884814; fax: +86 27 67883733.

E-mail address: yujunliang@sohu.com (Yujun Liang)

Experimental section

1. Chemicals

Zinc chloride ($ZnCl_2$), indium chloride ($InCl_3$) and thioacetamide (TAA) were purchased from Shanghai Macklin Biochemical Co., Ltd. Ethanol and glycol were purchased from Sinopharm Chemical Reagent Co., Ltd, China. Molybdenum carbide (Mo_2C) was purchased from the Inno-chem Co, Beijing. Ultrapure water (Milli-Q) was used to prepare the aqueous solution. All the reagents were used without any further purification.

2. Synthesis of pristine $ZnIn_2S_4$ and $Mo_2C@ZnIn_2S_4$ Schottky junction

$Mo_2C@ZnIn_2S_4$ Schottky junction was fabricated via a one-step low-temperature oil bath method. Specifically, 1 mmol $ZnCl_2$, 2 mmol $InCl_3$, and 4 mmol TAA were added to a mixture of deionized water (40 mL) and glycerol (10 mL) and stirred for 30 min. Then, an appropriate amount of Mo_2C (denoted as MC) powder was added to the above transparent solution with ultrasonic dispersion for 10 min. Subsequently, the resulting mixture was transferred to an oil bath, heated to 80 °C, and kept for 2 h. After cooling, the obtained samples were collected by centrifugation, washed using water and ethanol, and dried at 60 °C overnight. The as-prepared $Mo_2C@ZnIn_2S_4$ samples with 0.5 wt%, 1.5 wt% and 3.0 wt% Mo_2C were labeled as 0.5%MC@ZIS, 1.5%MC@ZIS and 3.0%MC@ZIS, respectively. For comparison, the bare $ZnIn_2S_4$ sample (denoted as ZIS) was synthesized as well according to the above routine without the addition of MC.

3. Characterization methods

X-ray powder diffraction (XRD) patterns of the as-prepared samples were measured in

the range 10-70° (2θ) on an X-ray diffractometer (D8-FOCUS, Bruker, Germany) operating with Cu Kα radiation (λ = 1.5418 Å). The morphologies of the as-prepared samples were analyzed by field emission scanning electron microscope (FE-SEM, SU8010, Hitachi, Japan) and transmission electron microscope (TEM, Tecnai G2 T20, FEI, America). Meanwhile, the energy-dispersive X-ray spectroscopy (EDS) spectra and elemental mapping images were recorded on an EDAX Genesis, which was attached to the FE-SEM. X-ray photoelectron spectroscopy (XPS) data were acquired on a Thermo Fisher Scientific equipped with an Al Kα as the excitation source. The UV-vis diffuse reflectance spectra (DRS) were performed on an UV-2550PC spectrophotometer (Shimadzu Corporation, Japan). The photoluminescence (PL) spectra were conducted on a fluorescence spectrometer (Fluoromax-4P, Horiba Jobin Yvon, New Jersey, USA), which was equipped with a 150 W xenon lamp as the excitation source. The photoluminescence decay curves were examined by a Fluorescence Spectrometer (FLS 920, Edinburgh Instruments, Livingston, UK). Brunauer-Emmett-Teller (BET) surface area was tested using N_2 adsorption-desorption isotherm (ASAP 2460, Micromeritics). The ultraviolet photoelectron spectroscopy (UPS) data were measured on ThermoFisher ESCALAB 250Xi.

4. Photocatalytic H_2 evolution coupled with furfuraldehyde production

The cooperative experiments of photocatalytic H_2 evolution and furfuraldehyde production were conducted in a sealed online automatic detection system (Labsolar-6A, Beijing Perfect Light Technology, China). Typically, 50 mg as-prepared photocatalyst

powder was dispersed into the 100 mL of a mixed aqueous solution containing 10 mL of furfuryl alcohol in a quartz reactor, and then sonicated for 0.5 h and vacuumed for 30 min to fully remove air. The temperature of the reaction system was maintained at 10 ºC through circulating cooling water, and the light source was a 300 W Xenon lamp (PLS-SXE300, Beijing Perfect Light Technology, China) equipped with a 420 nm cut-off filter. With continuous light irradiation for 4 h, the generated H_2 was collected at the given time intervals and quantitatively analyzed by gas chromatography (GC9560, TCD detector) with Ar as the carrier gas. Meanwhile, the yields of liquid products were detected by UV-Vis spectrophotometer at 278 nm.

5. Electrochemical measurements

The photocurrent response spectroscopy, electrochemical impedance spectroscopy (EIS) and Mott-Schottky plots were collected on a standard three-electrode electrochemical analyzer (CHI760E, Shanghai). The as-prepared sample coated onto the FTO electrode was served as the working electrode, an Ag/AgCl (saturated KCl) as the reference electrode, and a Pt foil as the counter electrode. The Na_2SO_4 (0.1 M) solution and 300 W Xe lamp (equipped with a 420 nm cut-off filter) were employed as electrolyte and light source, respectively. The working electrodes were prepared according to the previously reported method[S1]: 5 mg of photocatalyst powder and 10 μL of Nafion solution (5 wt%) were dispersed into 100 μL isopropanol and 300 μL water, and then ultrasonic treatment for 1 h to prepare a homogeneous catalyst colloid. Finally, the resultant catalyst slurry was coated onto the precleaned FTO glass surface with an active area of ca. 1.00 cm ×

1.00 cm and then dried in air.

6. Electron spin resonance Tests

The electron spin resonance (ESR) signal of the radical spin-trapped by 5,5- dimethyl-1-pyrroline-N-oxide (DMPO) was measured on a Bruker EMXPLUS spectrometer. The sample (10 mg) was dispersed in 2 mL furfuryl alcohol to form a uniform dispersion. A 300 W Xe arc lamp with a filter to cut off light of wavelength $\lambda < 420$ nm was used as the irradiation source. The 200 μL dispersion and 20 μL DMPO were mixed for the detection of carbon-centered radical.

Characterizations

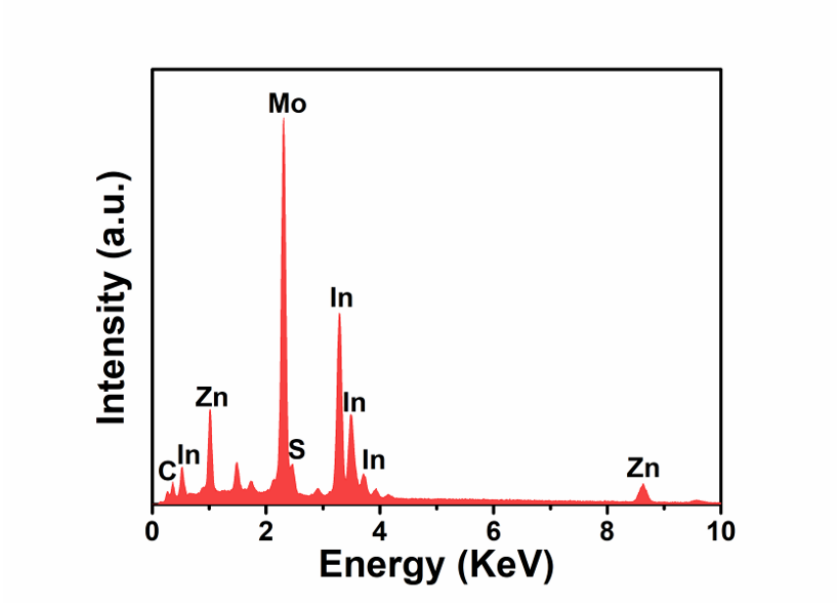

Fig. S1 EDS spectrum of 1.5%MC@ZIS sample.

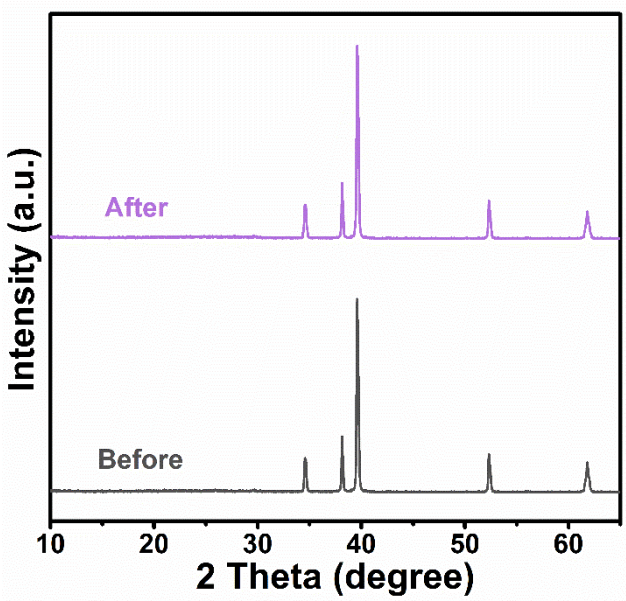

Fig. S2 XRD patterns before and after the oil bath process of MC.

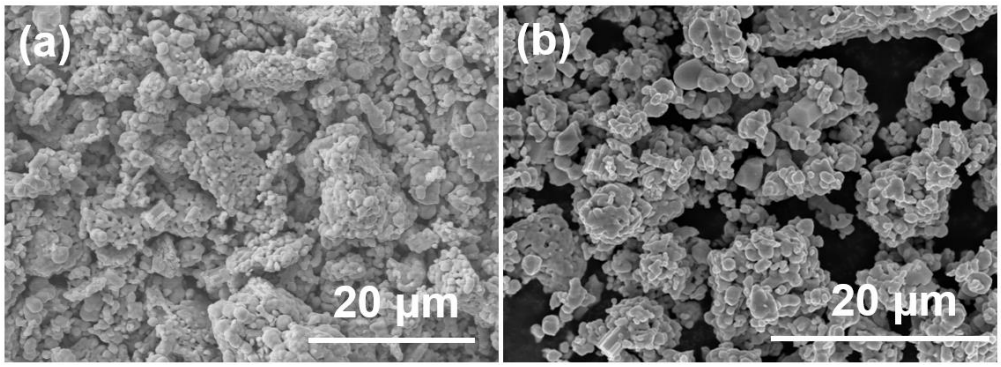

Fig. S3 SEM images (a) before and (b) after the oil bath process of MC.

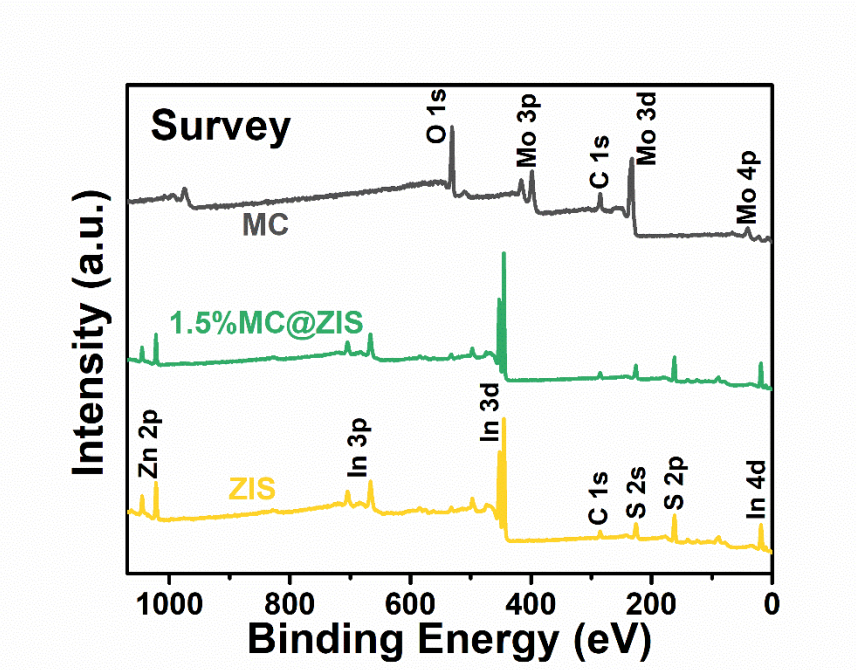

Fig. S4 XPS survey spectra of the as-prepared samples.

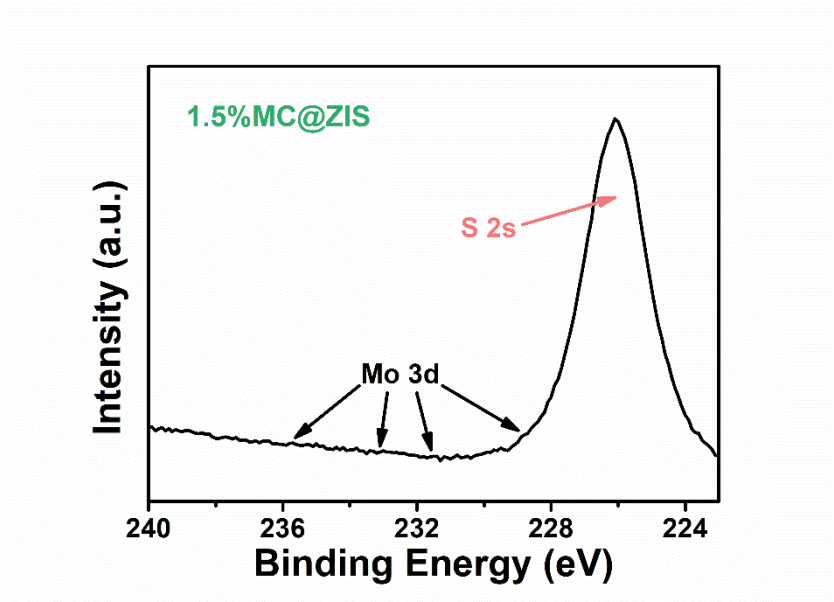

Fig. S5 Mo 3d and S 2s high-resolution XPS spectra of 1.5%MC@ZIS sample.

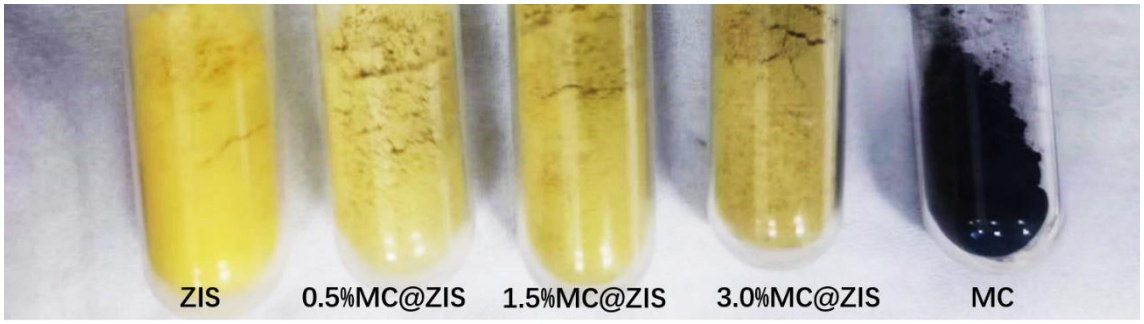

Fig. S6 The digital photographs of the as-prepared samples.

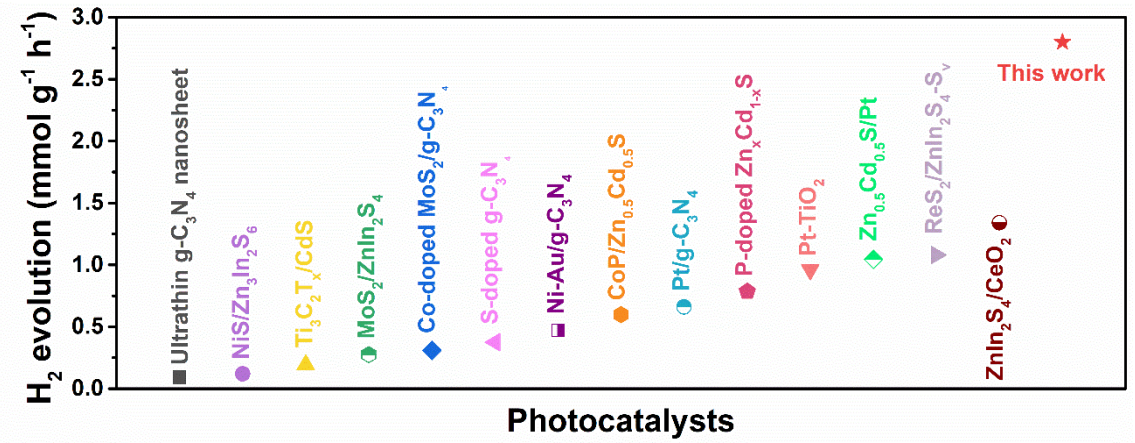

Fig. S7 Comparison of photocatalytic H_2 yield rates with previous reports in the analogous integrated photo-redox reaction systems.

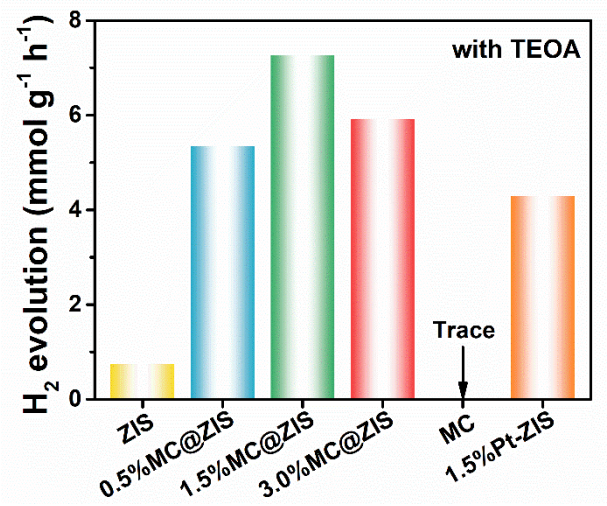

Fig. S8 The corresponding H_2 production rates of different samples in the aqueous solution of TEOA.

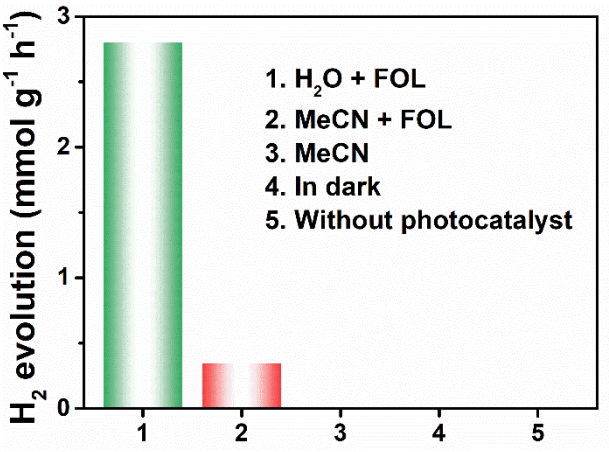

Fig. S9 Photocatalytic H_2 production rates of the prepared 1.5%MC@ZIS Schottky junction under different reaction conditions.

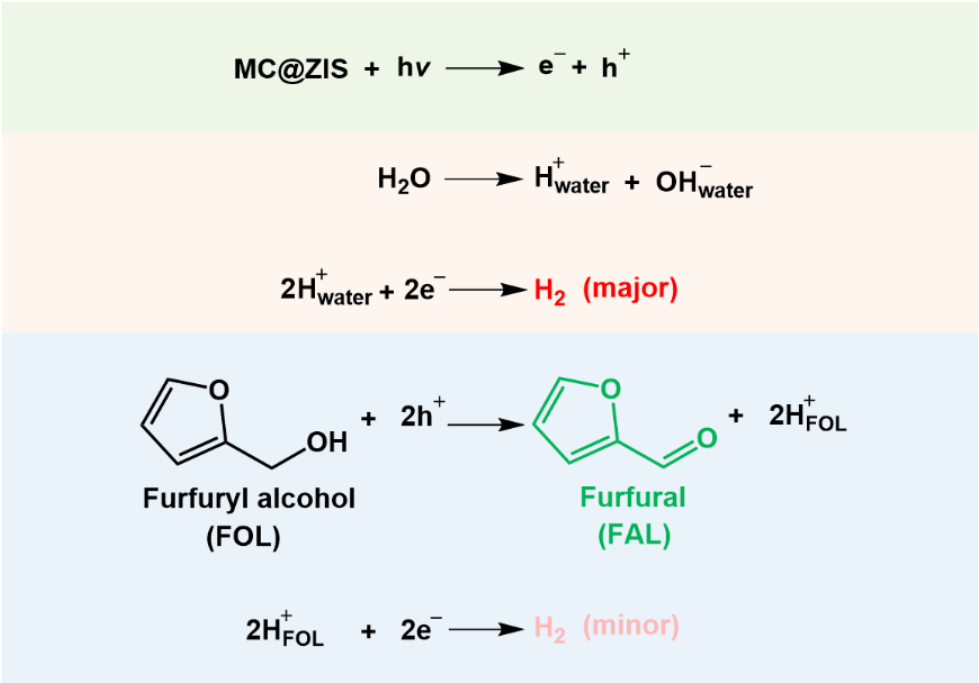

Fig. S10 The formulas of photo-redox dual reactions for integrating H_2 evolution and the FAL production.

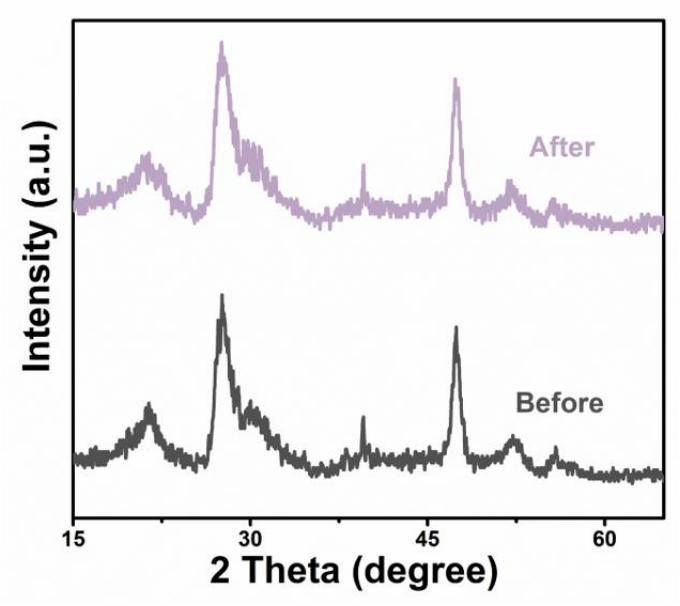

Fig. S11 XRD patterns before and after the photocatalytic cyclic experiments over 1.5%MC@ZIS.

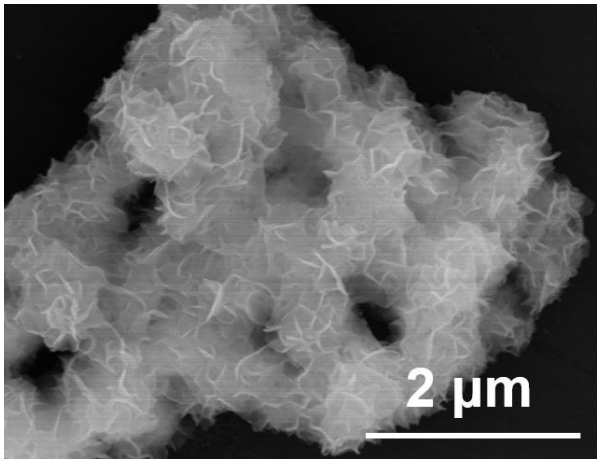

Fig. S12 SEM image of 1.5%MC@ZIS after the photocatalytic cyclic experiments.

Table S1 Comparison of photocatalytic H_2 production performance with previous reported photocatalysts in cooperative photo-redox reaction systems.

Samples	Reaction Conditions	Light Source	H_2 yield rate ($\mu mol\ g^{-1}\ h^{-1}$)	Ref.
Ultrathin g-C_3N_4 nanosheet	Aqueous solution (100 mL, 10 mM HMF, 3wt % Pt)	300 W Xe lamp ($\lambda > 420$ nm)	92	[S2]
NiS/$Zn_3In_2S_6$	Aqueous solution (50 mL, 0.1 M HMF)	300 W Xe lamp ($\lambda > 400$ nm)	120	[S3]
$Ti_3C_2T_x$/CdS	Aqueous solution (10 mL, 25 μmol FOL)	300 W Xe lamp ($\lambda > 420$ nm)	193.25	[S4]
MoS_2/$ZnIn_2S_4$	Aqueous solution (10 mL, 0.1 mmol FFA)	300 W Xe lamp ($\lambda > 420$ nm)	275.2	[S5]
Co-doped MoS_2/ g-C_3N_4	Aqueous solution (80 mL, 8 mL BA)	80 W LED lamp ($\lambda = 420$ nm)	310	[S6]
S-doped g-C_3N_4	Aqueous solution (20 mL, 21 μL BA)	300 W Xe lamp ($\lambda > 420$ nm)	376	[S7]
Ni-Au/g-C_3N_4	Aqueous solution (30 mL, 10 mM FOL)	Xe lamp (200 mW cm^{-2})	471.35	[S8]
CoP/$Zn_{0.5}Cd_{0.5}S$	Aqueous solution (50 mL, 0.1 mol/L HMF)	300 W Xe lamp ($\lambda > 400$ nm)	598	[S9]
Pt/g-C_3N_4	Aqueous (10 mL, 25 μmol 4-MBA), 0.08 mM Ru_{Cat}	300 W Xe lamp ($\lambda > 420$ nm)	660	[S10]
P-doped $Zn_xCd_{1-x}S$	Aqueous solution (2 mg/mL HMF)	30×3 W white LED light sources	786	[S11]
Pt-TiO_2	Acetonitrile solution (50 μmol BA)	UV LED (λ_{max} = 366 nm)	960	[S12]
$Zn_{0.5}Cd_{0.5}S$/Pt	Aqueous solution (40 mL, 5 μL FOL)	300 W Xe arc lamp	1045	[S13]
ReS_2/$ZnIn_2S_4$-S_v	Aqueous solution (100 mL, 3% (v/v) FOL, 1 wt% $H_2PtCl_6{\cdot}6H_2O$)	300 W Xenon lamp	1080	[S14]
$ZnIn_2S_4$/CeO_2	Aqueous solution (100 mL, 10 mL FOL)	300 W Xe lamp ($\lambda > 400$ nm)	1340	[S15]
Mo_2C@$ZnIn_2S_4$	**Aqueous solution (100 mL, 10 mL FOL)**	**300 W Xe lamp ($\lambda > 420$ nm)**	**2800**	**This work**

Notes: FOL = furfuryl alcohol; HMF = 5-hydroxymethylfurfural; 4-MBA = 4-methoxybenzyl alcohol; BA = benzyl alcohol.

References

[S1] G.G. Liu, G.X. Zhao, W. Zhou, Y.Y. Liu, H. Pang, H.B. Zhang, D. Hao, X.G. Meng, P. Li, T. Kako and J.H. Ye, In situ bond modulation of graphitic carbon nitride to construct p-n homojunctions for enhanced photocatalytic hydrogen production, *Adv. Funct. Mater.*, 2016, **26**, 6822-6829.

[S2] X. Bao, M. Liu, Z. Wang, D. Dai, P. Wang, H. Cheng, Y. Liu, Z. Zheng, Y. Dai and B. Huang, Photocatalytic selective oxidation of HMF coupled with H_2 evolution on flexible ultrathin g-C_3N_4 nanosheets with enhanced N-H interaction, *ACS Catal.*, 2022, **12**, 1919-1929.

[S3] S. Meng, H. Wu, Y. Cui, X. Zheng, H. Wang, S. Chen, Y. Wang and X. Fu, One-step synthesis of 2D/2D-3D NiS/$Zn_3In_2S_6$ hierarchical structure toward solar-to-chemical energy transformation of biomass-relevant alcohols, *Appl. Catal. B Environ.*, 2020, **266**, 118617.

[S4] Y.H. Li, F. Zhang, Y. Chen, J.Y. Li and Y.J. Xu, Photoredox-catalyzed biomass intermediate conversion integrated with H_2 production over $Ti_3C_2T_x$/CdS composites, *Green Chem.*, 2020, **22**, 163-169.

[S5] C.L. Tan, M.Y. Qi, Z.R. Tang and Y.J. Xu, Cocatalyst decorated $ZnIn_2S_4$ composites for cooperative alcohol conversion and H_2 evolution, *Appl. Catal. B Environ.*, 2021, **298**, 120541.

[S6] Y. Hu, X. Yu, Q. Liu, L. Wang and H. Tang, Highly metallic Co-doped MoS_2 nanosheets as an efficient cocatalyst to boost photoredox dual reaction for H_2 production and benzyl alcohol oxidation, *Carbon*, 2022, **188**, 70-80.

[S7] F. Zhang, J. Li, H. Wang, Y. Li, Y. Liu, Q. Qian, X. Jin, X. Wang, J. Zhang and G. Zhang, Realizing synergistic effect of electronic modulation and nanostructure engineering over graphitic carbon nitride for highly efficient visible-light H_2 production coupled with benzyl alcohol oxidation, *Appl. Catal. B Environ.*, 2020, **269**, 118772.

[S8] Q. Yang, T. Wang, F. Han, Z. Zheng, B. Xing and B. Li, Bimetal-modified g-C_3N_4 photocatalyst for promoting hydrogen production coupled with selective oxidation of biomass derivative, *J. Alloys Compd.*, 2022, **897**, 163177.

[S9] Y. Yang, W. Ren, X. Zheng, S. Meng, C. Cai, X. Fu and S. Chen, Decorating $Zn_{0.5}Cd_{0.5}S$ with C,N Co doped CoP: An efficient dual-functional photocatalyst for H_2 evolution and 2,5-Diformylfuran oxidation, *ACS Appl. Mater. Interfaces*, 2022, **14**, 54649-54661.

[S10] F. Li, Y. Wang, J. Du, Y. Zhu, C. Xu and L. Sun, Simultaneous oxidation of alcohols and hydrogen evolution in a hybrid system under visible light irradiation, *Appl. Catal. B Environ.*, 2018, **225**, 258-263.

[S11] H.F. Ye, R. Shi, X. Yang, W.F. Fu and Y. Chen, P-doped $Zn_xCd_{1-x}S$ solid solutions as photocatalysts for hydrogen evolution from water splitting coupled with photocatalytic oxidation of 5-hydroxymethylfurfural, *Appl. Catal. B Environ.*, 2018, **233**, 70-79.

[S12] K. Imamura, H. Tsukahara, K. Hamamichi, N. Seto, K. Hashimoto and H. Kominami, Simultaneous production of aromatic aldehydes and dihydrogen by photocatalytic dehydrogenation of liquid alcohols over metal-loaded titanium(IV) oxide under oxidant- and solvent-free conditions, *Appl. Catal. A Gen.*, 2013, **450**, 28-33.

[S13] Z. Wang, L. Wang, B. Cheng, H. Yu and J. Yu, Photocatalytic H_2 evolution coupled with furfuralcohol oxidation over Pt-Modified ZnCdS solid solution, *Small Methods*, 2021, **5**, 2100979.

[S14] J. Hu, X. Li, J. Qu, X. Yang, Y. Cai, T. Yang, F. Yang and C.M. Li, Bifunctional honeycomb hierarchical structured 3D/3D $ReS_2/ZnIn_2S_4$-S_v heterojunction for efficient photocatalytic H_2-evolution integrated with biomass oxidation, *Chem. Eng. J.*, 2023, **453**, 139957.

[S15] G. Zhang, S. Huang, X. Li, D. Chen, N. Li, Q. Xu, H. Li and J. Lu, Internal electric field engineering of bifunctional 2D/2D heterojunction photocatalyst for cooperative H_2 production and alcohol conversion, *Appl. Catal. B Environ.*, 2023, **331**, 122725.